Lab on a Chip

Micro- & nano- fluidic research for chemistry, physics, biology, & bioengineering

www.rsc.org/loc

Volume 10 | Number 12 | 21 June 2010 | Pages 1493–1632

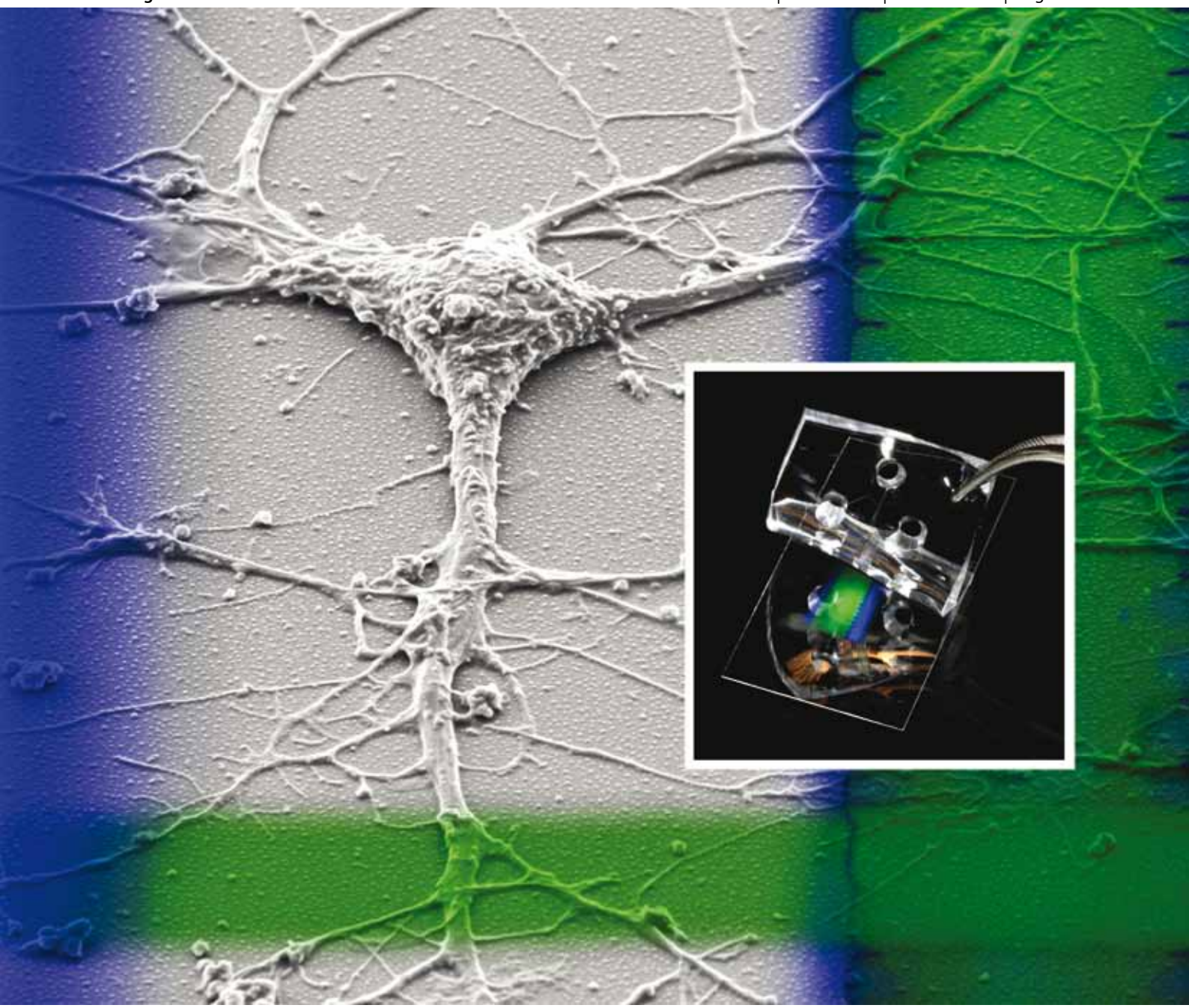

ISSN 1473-0197

RSC Publishing

Gillette
Guiding neuron development

Muller and Sohn
Single-molecule sequencing

Celebrating 10 Years of publishing

1473-0197(2010)10:12;1-8

Guiding neuron development with planar surface gradients of substrate cues deposited using microfluidic devices†

Larry J. Millet,[a] Matthew E. Stewart,[b] Ralph G. Nuzzo[b] and Martha U. Gillette*[a]

Received 25th January 2010, Accepted 23rd March 2010
First published as an Advance Article on the web 13th April 2010
DOI: 10.1039/c001552k

Wiring the nervous system relies on the interplay of intrinsic and extrinsic signaling molecules that control neurite extension, neuronal polarity, process maturation and experience-dependent refinement. Extrinsic signals establish and enrich neuron–neuron interactions during development. Understanding how such extrinsic cues direct neurons to establish neural connections *in vitro* will facilitate the development of organized neural networks for investigating the development and function of nervous system networks. Producing ordered networks of neurons with defined connectivity *in vitro* presents special technical challenges because the results must be compliant with the biological requirements of rewiring neural networks. Here we demonstrate the ability to form stable, instructive surface-bound gradients of laminin that guide postnatal hippocampal neuron development *in vitro*. Our work uses a three-channel, interconnected microfluidic device that permits the production of adlayers of planar substrates through the combination of laminar flow, diffusion and physisorption. Through simple flow modifications, a variety of patterns and gradients of laminin (LN) and fluorescein isothiocyanate-conjugated poly-L-lysine (FITC–PLL) were deposited to present neurons with an instructive substratum to guide neuronal development. We present three variations in substrate design that produce distinct growth regimens for postnatal neurons in dispersed cell cultures. In the first approach, diffusion-mediated gradients of LN were formed on cover slips to guide neurons toward increasing LN concentrations. In the second approach, a combined gradient of LN and FITC–PLL was produced using aspiration-driven laminar flow to restrict neuronal growth to a 15 μm wide growth zone at the center of the two superimposed gradients. The last approach demonstrates the capacity to combine binary lines of FITC–PLL in conjunction with surface gradients of LN and bovine serum albumin (BSA) to produce substrate adlayers that provide additional levels of control over growth. This work demonstrates the advantages of spatio-temporal fluid control for patterning surface-bound gradients using a simple microfluidics-based substrate deposition procedure. We anticipate that this microfluidics-based patterning approach will provide instructive patterns and surface-bound gradients to enable a new level of control in guiding neuron development and network formation.

Introduction

Microfabrication technologies have been used to chemically and topologically pattern glass cover slips to investigate the influences of such features on neuronal polarity, axon migration and growth cone behaviors. Microfluidic devices have been employed in studies of: axon regeneration,[1] positioning neurons in micro-devices,[2] integrating networks of neurons with multielectrode arrays,[3] and confining neurites for axon-selective mRNA analysis.[4] The application of microfluidics in neuroscience is still young, nevertheless, this technology has made significant contributions in many areas.

Patterned substrates have been used for defining and regulating extrinsic cues in order to direct neuronal growth and polarity.[5–8] In the brain and *in vitro*, neurons contact surfaces for stabilizing attachment and, importantly, for receiving developmentally instructive signals that are transduced to modulate gene transcription, energy/resource utilisation, and neuronal fine structure mediated through the cytoskeleton.[9,10] Microfluidic devices can be used to form binary chemical patterns that can be used to present cells with stark differences in the substratum.[8] Patterns can be deposited using microcontact printing,[7,11–13] but this process is challenging and inefficient for substrate gradients.

To investigate substrate-mediated axo-dendritic polarity, Banker and colleagues presented hippocampal neurons with patterned stripes of defined bioactive cell adhesion molecules. Their work showed the ability to juxtapose substrates that induce axo-dendritic specification of differentiating primary neurites *in vitro*.[8] Through extensions of this approach, intersecting lines of different recombinant cell adhesion molecules further refined the analysis of neurite navigation *in vitro*.[7] The implementation of patterned substrates for neurobiological studies has demonstrated that various immobilized, bioactive substrates

[a]*Department of Cell and Developmental Biology, University of Illinois at Urbana-Champaign, Urbana, IL, 61801, USA. E-mail: mgillett@illinois.edu; Tel: +1-217-244-1355*
[b]*Department of Chemistry and the Frederick Seitz Materials Research Laboratory, University of Illinois at Urbana-Champaign, Urbana, IL, 61801, USA. E-mail: r-nuzzo@illinois.edu*

† Electronic supplementary information (ESI) available: Supporting neuron images. See DOI: 10.1039/c001552k

predictably guide neuron development,[6,11,13,14] polarization,[8,12] axon migration,[7] and growth cone navigation.[6] Because trophic factors have a beneficial role in development, they can be immobilized as patterned substrates for activating neurons and regulating development through surface contacts.[15–17]

While developmental studies using planar patterns have provided insights on directed neurite development, neuronal differentiation is influenced by both surface-bound and diffusive gradients of extrinsic signaling molecules. Keenan and Folch review the benefits and limitations of many of the approaches for producing biomolecular gradients *in vitro*.[18] Traditional approaches for years have produced effective, non-quantitative gradients, while newer approaches utilize microtechnology to yield more precisely regulated and quantifiable fluidic-based gradients. Both approaches are valuable, and selecting the appropriate method requires understanding the constraints and demands of the biological question.

Polydimethylsiloxane (PDMS) is a widely used material for fabricating microfluidic devices, principally due to its affordability, ease of fabrication and use, and general biocompatibility.[19–21] Microfluidics approaches improve spatiotemporal fluidic control of the microenvironment to which the neuron is exposed,[22] provide a physical barrier that confine neurites,[1,4,23] enable control of neural network connectivity,[24,25] and facilitate the manipulation and processing of minuscule sample volumes of cellular analytes for biochemical analysis.[26–31] The present work exploits these qualities and joins them more generally to the patterning capabilities of soft lithographic/microfluidic patterning.

Laminin (LN) and growth factors are instructive elements of the extracellular matrix and an axon permissive cue for orienting neurons and establishing neuronal polarity.[8,32–39] Microfluidic devices can be used to generate useful gradients of LN to promote neurite guidance[37] and growth factor gradients that optimize the proliferation and differentiation of human neural stem cells.[40] Microfluidic channels also can be designed in a range of sizes and complexities to incorporate valves for flow actuation and to sustain tunable solution-phase gradient forms for tuning, *via* real-time manipulation, fluid-phase diffusive gradients.[18,41–45] While complex, state-of-the-art microfluidics provide capacities for programmatic switching, and flow manipulation can be exceptionally empowering, studies examining primary neurons *in vitro* do not necessarily require advanced capacities of this type, and may suffer from them. The pressures and flow rates applied through dynamically actuated microfluidic devices, in many cases, induce flow-field forces (*e.g.*, shear stresses)[46–50] that influence the structure and function of the cell.[46,51–54] Flow-field stresses can negatively bias the micron-scale neurites, the neuronal responses or prove altogether fatal. For these reasons, specialized device designs have been engineered to provide the necessary requirements for fluid mass transfer without inflicting flow-based artefacts.[50]

Alternative microdevice designs have established more permissive means for gradient generation. These include the general competency of diffusion-field patterning,[55,56] the cross-channel,[57,58] and microjet approaches.[59] These latter methods provide a significant advantage in that they enable substrate gradient formation while eliminating the cellular impacts of shear effects that accrue at high flow velocities.[49]

In this work, we specifically focus on controlling the substratum by patterning surface-bound gradients using the spatiotemporal fluidic control afforded by microfluidics for guiding neuron development *in vitro*. Here, the benefits of laminar flow and diffusion are combined through the use of interconnecting microchannels to provide an efficient means of patterning proteinaceous cues on glass surfaces. Our results show that this surface patterning approach is compliant with, and meets the biological requirements for, controlling mammalian neuron development. This patterning approach is broadly applicable to cell biology and is compatible with the traditional cultures of primary neurons in Petri dishes and on cover slips.

Methods

Microfluidic device fabrication

The schematic in Fig. 1 shows the general process for microfluidic device fabrication and its use for patterning cover slips for cell cultures. Microfluidic devices with multi-height channels are formed by casting and curing PDMS against a master consisting of a silicon wafer supporting multi-height photoresist features.

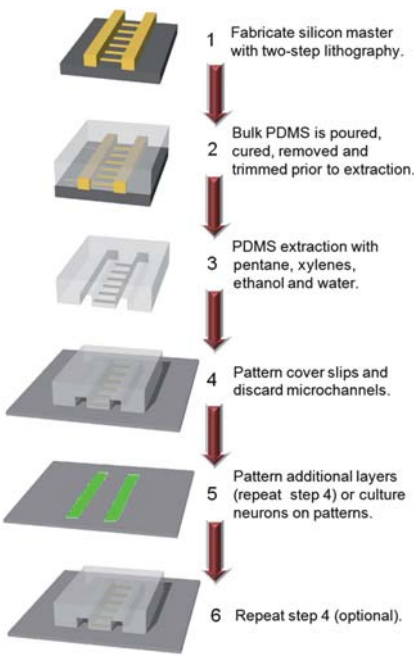

Fig. 1 Fabrication of microfluidic devices for patterning substrates for neuronal cultures. *Step 1*: master fabrication using photolithography: a master consisting of multi-height photoresist features on a silicon wafer was fabricated using standard lithography. The primary channels range from 50–200 μm by ~45 μm; smaller interconnects are 3–7 μm by 3 μm, width by height, respectively. *Step 2*: PDMS pre-polymer is poured onto the masters, cured at 70 °C for 2 h, removed from masters and trimmed of excess PDMS prior to solvent extraction. *Step 3*: PDMS microfluidic channels are solvent-extracted with pentane, xylenes, ethanol and water.[23] *Step 4*: planar-patterned binary lines or substrate gradients are formed on glass cover slips by laminar flow and diffusion. *Step 5*: channels can be removed to form planar, surface-bound substrate gradients on cover slips for two-dimensional neuronal cultures. *Step 6*: additional microchannel structures can be assembled onto the patterned cover slip for further patterning of multiple substrate layers.

Table 1 Dimensions of each type of microdevice in the library of devices used for substrate patterning

	Primary channels			Interconnecting channels		
Device type	Channel 1 width/μm	Channel 2 width/μm	Channel 3 width/μm	Length/μm	Width/μm	Height/μm
A1	200	200	200	35–40	2–3	3
A2	50	200	50	35–40	2–3	3
A3	200	50	200	35–40	2–3	3
B1	200	200	200	35–40	7–10	3
B2	50	200	50	35–40	7–10	3
B3	200	50	200	35–40	7–10	3

Table 1 outlines the six different channel designs used in this work. *Step 1*: two sequential photolithographic processes are used to make masters with multi-height photoresist features. The small parallel 'interconnect' channels are first formed using SU-8 (2) spun in a thin layer (~3 μm) followed by exposure through a high-resolution quartz/chromium mask (defined by electron beam lithography). The three larger parallel channels are then formed by casting a thicker layer (~45 μm) of SU-8 (50) on the master followed by exposure through a transparency mask (defined by ink-jet printing) that is aligned with the small interconnect channels formed during the first step. Resist spinning, exposure and baking are performed as directed by the manufacture's specifications. As described previously,[23] masters are passivated with a layer of (tridecafluoro-1,1,2,2-tetrahydrooctyl)trichlorosilane to facilitate PDMS release. *Step 2*: PDMS pre-polymer (Sylgard 184, Dow Corning) is poured to a thickness of 2–4 mm on the master and cured at 70 °C for 2 h and stored in ambient conditions (~25 °C) until used. *Step 3*: prior to use for cover slip patterning or cell culture, PDMS channels are extracted in solvents to remove residual, uncrosslinked components, producing extracted PDMS (E-PDMS) from the PDMS. Unextracted PDMS is known to interfere with neuron cultures[23] and leaves residues on surfaces upon contact,[60–66] whereas E-PDMS exhibits greatly improved biocompatibility and minimizes surface residues.

The extraction protocol (Step 3) has been shortened from our previous work.[23] E-PDMS is prepared by submerging devices measuring approximately 464 mm^2 and 2–4 mm thick in 150–200 mL of the following solvents for the indicated times: HPLC-grade pentane (Fisher Scientific) for ~16 h; xylenes isomers plus ethylbenzene 98.5+% (xylenes) (Sigma) for 1–2 h; xylenes for 2–4 h; 200 proof ethanol (EtOH) USP for 1–2 h (AAPER); EtOH for at least 2 h, and, finally, the PDMS channels are submerged in 1 L of sterile DI water overnight and dried prior to use.

Cover slip patterning

Planar-patterned gradients. *Step 4*: the E-PDMS channels are attached to the cover slips *via* conformal contact. Then, planar-patterned gradients on acid-cleaned cover slip surfaces are formed by flowing solutions of selected chemical cues through the E-PDMS channels attached to the glass substrates.[23] Laminin (LN) (Invitrogen, Carlsbad, CA), fluorescein isothiocyanate-conjugated poly-L-lysine (FITC–PLL) (Sigma, St Louis, MO), and Texas Red-conjugated bovine serum albumin (TR–BSA) (Molecular Probes, Eugene, OR) are diluted to 100 μg mL^{-1} in phosphate buffered saline (PBS, 0.1 M, pH 7.4). For channel patterning, all solutions are filtered through 0.22 μm filters to yield fluids free of debris. In general, substrate solutions were perfused through the three large primary channels prior to cell culture with the order, duration, and flow necessary to enable controlled exposure of the solutions to the glass substrate. Microfluidic assembly for patterning and culture can be repeated for combining patterns or gradients on a 2-D cover slip.

Step 5: to view the LN pattern, the cover slip is immunochemically labeled with polyclonal antibodies that recognize LN.[37] While the LN-patterned source channel could easily be identified, the immunofluorescence from the laminin-patterned diffusion field is insufficient for characterizing the slope and width of the surface gradient cue; therefore, we rely on the inherent ability of neurons to sense the change in LN concentration and respond to their extracellular domain. To avoid confounding variables that could be attributed to PDMS footprints or residues left on the cover slip where the PDMS made contact with the cover slip, all patterning processes in this work are performed using E-PDMS. Residual PDMS oligomers that could be deposited through contact of PDMS to the glass[60,62,63,67–70] were minimized in this way. It is possible that the micron-scale foot print from the PDMS interconnects could act as a navigational cue; however, under these gradient forms, the LN cue guides the axons up the diffusion field toward the LN source to orient the navigation of axons apart from any cue the footprint may provide.

Binary patterned lines. For binary patterned lines formed in conjunction with surface gradients, parallel non-interconnecting microchannels are brought into conformal contact with acid-cleaned cover slips prior to gradient formation. FITC–PLL is briefly perfused through the channels, then flow is stopped and the lysine–polymer solution is allowed to incubate on the glass in the channel for approximately 5–10 min. Care is taken to avoid excess coating outside the channel array to avoid unnecessary coating of the glass. The FITC–PLL is aspirated and the channels and cover slip rinsed thoroughly using sterile DI water. Then, the cover slip and channels are aspirated until dry wherein the PDMS channels are removed and discarded (Steps 4 and 5). Gradients can be formed by repeating the patterning process on the binary lines (Step 6).

Cell culture

For postnatal (P1–P2) hippocampal neurons, Long-Evans Blu-Gill rats (University of Illinois at Urbana-Champaign) were used in accordance with protocols established by the University of

Illinois Institutional Animal Care and Use Committee and in accordance with all state and federal regulations.

Primary hippocampal neurons. Tissue from P1–P2 is harvested following our previously published protocol;[23] Hibernate-A (Brain Bits, Springfield, IL) and Neurobasal-A without phenol red (Invitrogen), supplemented with 0.5 mM L-glutamine, B-27, 100 U mL^{-1} penicillin and 0.1 mg mL^{-1} streptomycin, are used for isolation and culture, respectively. Animals are rapidly decapitated, the brain removed and hippocampi dissected in ice-cold Hibernate. Hippocampi are pooled and treated with papain (25.5 U mL^{-1}) in Hibernate for 30 min at 37 °C. Following papain treatment, the enzyme-containing solution is aspirated and hippocampi are rinsed with 1 mL of enzyme-free Hibernate. Cells are then mechanically dissociated through trituration in 2 mL Hibernate using a fire-polished Pasteur pipette. After undissociated tissue settles, the supernatant is transferred to a new 15 mL vial and the process repeated. The resulting supernatant is combined and centrifuged at 1400 rpm for 5 min. Cells are resuspended, counted, diluted in Neurobasal media, and plated at 100–125 cells mm^{-2} for two-dimensional cultures without microchannels.

Immunochemistry

Immunolabeling patterned laminin. For imaging LN patterns with living neurons cultivated on the substrate, or patterned glass without neurons (Fig. 1, Step 5), primary rabbit polyclonal antibodies against LN (1 : 1–2000, Sigma) are introduced directly into the culture media of live hippocampal neuron cultures and incubated for 20 min in the incubator; as the B-27 supplement contains an abundance of albumin, a separate blocking step was not necessary. The culture media with LN antibodies are carefully removed from the dish and the cells are gently rinsed with pre-warmed culture media containing secondary antibodies (Alexa 350 (blue) or Alexa 568 (red) goat anti-rabbit, 1 : 1000, Invitrogen) against the LN polyclonal antibody and returned to the incubator for another 20 min. Finally, the media with secondary antibody are removed and the living cells are rinsed with 10% glycerol in PBS (37 °C) to stabilize the neurons and the micron-scale axons during imaging. Glycerol stabilization greatly extends the ability to study and image live neurons for our analysis. Because the fixation process can attenuate or eliminate the fluorescence of conjugated substrates, fixation was not used and neurons were evaluated using live cell imaging.

Immunocytochemistry of cell cultures. For fixing and labeling neurons on the cover slip, cells are fixed with 4% paraformaldehyde or gluteraldehyde in PBS for 30 min, permeabilized with 0.25% Triton in PBS, and blocked at room temperature with 5% normal goat serum (NGS) in PBS. Primary and secondary antibodies are incubated with 2.5% NGS in PBS. Monoclonal mouse primary antibodies are against α-tubulin (1 : 1000, Sigma), and the rhodamine-conjugated phalloidin labeled filamentous actin (1 : 1000, Molecular Probes). Following antibody labeling, samples are rinsed with PBS then imaged with PBS for immediate imaging; alternatively, samples are rinsed with DI water, dehydrated, and mounted with Prolong Gold anti-fade reagent (Molecular Probes) before imaging to prevent photobleaching.

Microscopy and data analysis

Planar-patterned cover slips are imaged on a laser-equipped Zeiss LSM-510 Meta NLO[23] or a Zeiss Axiovert 200M fluorescence microscope with mercury lamp illumination (X-Cite series 120) and an Axiocam MRm with Axiovision software. Substrate gradient intensity profiles are acquired with the Zeiss LSM acquisition software. Neurite traces for quantitation are performed with Neurolucida and Neurolucida Explorer and displayed in the polar histogram.

For determining the instructive nature of 2-D, surface bound LN gradients, all putative neurons in the gradient zone are classified and tallied for net axonal migration after 4 DIV. The mean and standard deviation of the percent of the neuronal population with categorical migration (orienting toward the LN source, parallel to the LN source channel, or away from the LN source) of all five patterned samples are displayed, as will be discussed below. Samples were inspected through microscopy for particulates or debris that produce 'broken' gradients or interrupted flow fields; affected samples were not used. Young neurons (4 DIV) are identified by morphological characteristics of this developmental stage, many short processes (dendrites) and one longer process (axon) that is at least 3-times longer than the shorter processes (Fig. S1†).[37] Traces of axons migrating toward LN are representative of the navigational trend; all neurons shown are from a single cover slip from the five replicates. Perikaryons are marked with a spot of the same color. The axons of all neurons within the gradient zone are traced until the branch point or axon was no longer discernible from another neuron. Neurite traces are performed by directly tracing the neurites of the images. Neurite traces are aligned to the gradient zone or displayed in the polar histogram.

Results and discussion

The device used in the current work simplifies the earlier designs in important ways while preserving capabilities to regulate mass transfer, and in that way to control gradient forms of patterning. The device design we used here contains three larger (50 or 200 μm wide) parallel channels (two peripheral, one central) that are fluidically connected *via* small micron-scale interconnecting channels (Fig. 2a). We fabricated a library of devices with a range of dimensions for the peripheral, central and interconnecting channels for use in patterning the cellular substrates (Table 1). These microfluidic devices confer the simultaneous and independent ability to control multiple fluidic domains for patterning and programming gradients of substrate cues *via* mechanisms exploiting both diffusive mass transfer and laminar flow dynamics.

Diffusion field patterning: laminin gradients orient neuron development

To better define the temporal parameters for surface-bound gradients in our system, we perfused the two peripheral channels with FITC–PLL while imaging the diffusive spread of the substrate fluorescence through the interconnecting channels

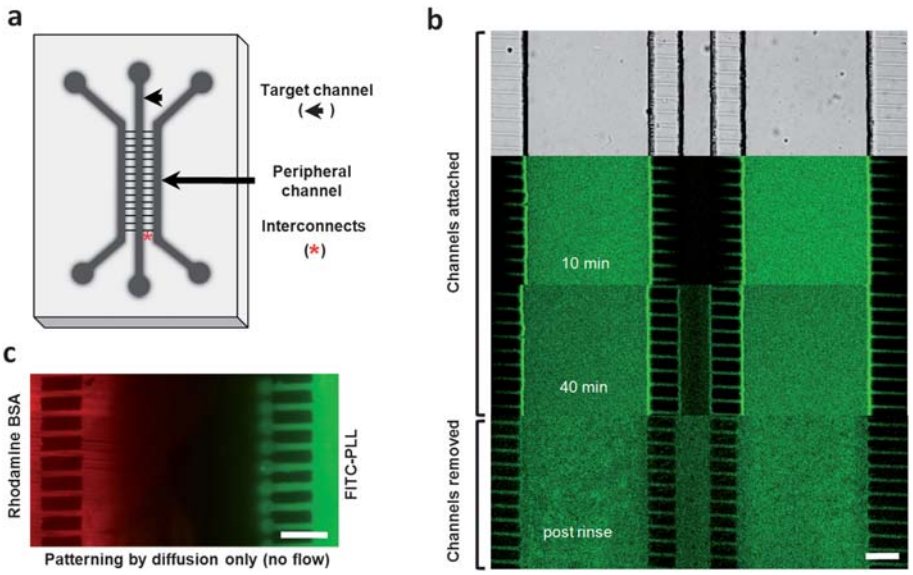

Fig. 2 Diffusion through microfluidic interconnects. (a) Schematic of the channel design used in this study. (b) Transmitted light image of channels and a time-lapse imaging sequence (confocal microscopy) of fluorescence images from a single device (type A3). After filling all channels with PBS, FITC–PLL was introduced into the side channels (200 μm) and imaged over a period of 40 min. FITC–PLL can be detected diffusing through interconnects and into the center channel. The post-rinse image shows that by 40 min the glass surface of the central channel has been uniformly coated with FITC–PLL. (c) An example of how two different substrates, Texas Red-conjugated bovine serum albumin (TR–BSA, red) and FITC–PLL (green) can coat glass differently based, in part, on the intrinsic molecular properties for diffusion and adsorption (device type A2). Gradients can be established by modulating the concentration of the substrate solution, incubation time, relative channel pressures (pumping technique used) and interconnecting channel dimensions or stamp architecture. Scale bars = 50 μm.

(Fig. 2b). Within the first 10 min, FITC–PLL diffused through the interconnects and emerged into the central channel; within 40 min the FITC–PLL permeated the target channel sufficiently to adsorb onto the glass with the same coverage as the source channels. We extended this approach to Texas Red-conjugated bovine serum albumin (TR–BSA), which demonstrated different glass-coating characteristics apart from FITC–PLL (Fig. 2c). As a result, chemical substrates can be deposited in a target channel by diffusion through fine interconnects, without flow, with the coverage and gradient extension modulated as a function of time.

We extended the diffusion-based approach to forming surface-bound gradients of LN. After pre-filling all channels with PBS, LN was aspirated into a single source channel and incubated for 5–10 min (Fig. 3a) to enable diffusion-mediated surface coating. To reduce extensive LN-mediated neuron clustering resulting from neuron migration, channels were post-rinsed with FITC–PLL (a promoter of cell adhesion) to add a FITC–PLL layer to the substrate pattern (Fig. 3b). In addition, the FITC–PLL layer also served to enable the visualisation, *via* live-neuron imaging, of the treated channel structures for assessing the effectiveness of the LN orientation on growth (Fig. 3d).

Axons of cultured primary hippocampal neurons growing on the diffusion zone navigate toward the LN source (Fig. 3c and e). Five samples from three separate patterning and culture experiments were analyzed; all neurons in the diffusion zone were classified (Fig. 3c) and tallied for net axonal migration after 4 days *in vitro* (DIV) (Fig. 3d). The population for each classification of axon migration arrow in the image is identified by blue ("W" toward LN), red ("N+S" indifferent to LN), or yellow ("E" away from LN), and corresponds to the colored data bars in the adjacent graph (Fig. 3d). In addition, "undetermined" cells were included ("Other", black data bar), accounting for the following: cells with processes but no defined axon (likely undifferentiated neurons), too many intersecting neurites masking the identification of the axon, or undifferentiated cells. The mean and standard deviation of the percent of the neuronal population with categorical migration are displayed with the respective orientation (Fig. 3d). Neurons show a repeatable, statistically significant preference for LN in response to substrate gradients of these diffusion fields, ($p \leq 0.0001$, unpaired t-test).

When the orientations of axonal processes of all neurons from a single representative culture responding to the LN gradient with a uniform FITC–PLL layer (plotted in Fig. 3c) are examined, interesting migration patterns are observed (Fig. 3e). One neuron migrates away from the LN source, while all others respond and orient toward LN. Axons on the LN pattern of the source channel have the capacity to migrate off of the LN source because of the uniform FITC–PLL layer. Fig. 4 shows that axons migrating down the laminin gradient formed distinct "U-turns" in the diffusion zone to return to the LN source channel. This axon guidance is not observed in control cultures of patterned FITC–PLL without LN gradient cues, where neurons develop long neurites that intermingle across all patterned areas indicative of random migration (Fig. S1†). This makes individual cell and neurite distinction difficult (Fig. 3f).

It is well established that LN is an effective cue for neurite navigation and outgrowth-promoting activity.[5,8,37,71] When dissociated hippocampal neurons are exposed to binary, alternating lines of LN and PLL, LN is a strong inducer of substrate directed axon specification and accelerated axon growth.[8] Further work capitalized on microfluidic gradient mixers to form stable, linear LN gradients for orienting axon specification

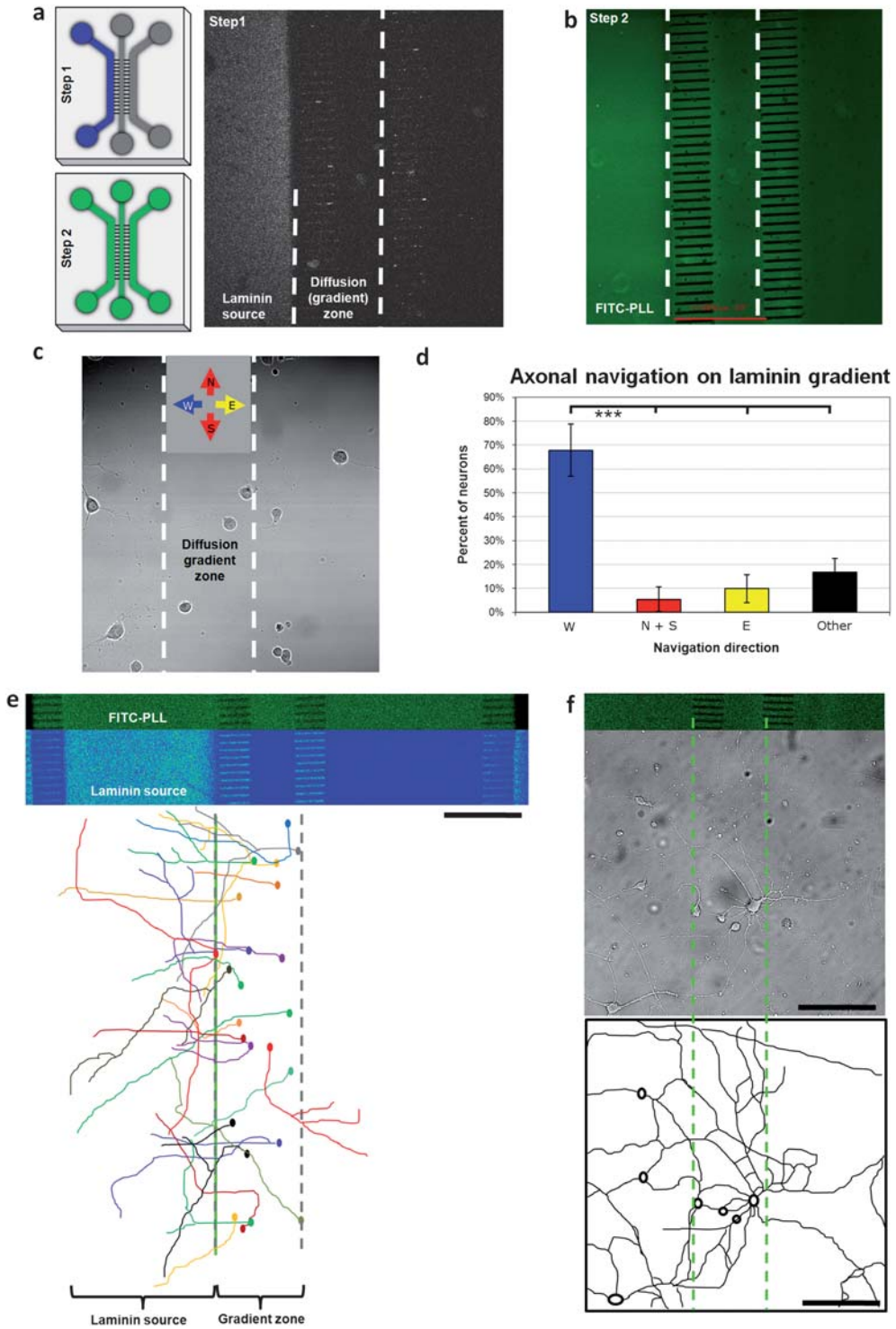

Fig. 3 Fabrication of single-component substrate gradients that guide neuron development. (a) The entire device (type B3) was filled with PBS, laminin (LN) introduced into one side-channel of the microfluidic device (Step 1). LN was identified through immunochemistry using Alexa 350-conjugated antibodies (blue). (b) All channels were rinsed with FITC–PLL (Step 2) followed by PBS, the channels were then removed and discarded. (c) Directional navigation was assessed for axons (the longest process) of all hippocampal neurons at 4 DIV within the diffusion zone of five gradient-patterned cover slips. (d) Navigation direction is represented graphically as mean ± standard deviation of population percentages. Neurons show a repeatable, statistically significant preference for LN ($p \leq 0.0001$, unpaired t-test). Colored arrows (c) correspond to the graph (d) depicting the primary axis of directed axonal growth (W, N+S, E, Other). Total neurons analyzed for each of 5 samples are 92, 27, 28, 27, and 16; (a, b, and d) transmitted light and fluorescent images shown are from a single, representative sample visualized by confocal and laser scanning microscopy, respectively. (e) Images of neurons and substrates and traces of neuronal processes from one of the five LN gradient samples and (f) from a control cover slip of patterned with FITC–PLL and without a LN gradient. On the sample without gradients, neurites frequently intermingle so as to disallow axonal distinction, as evidenced by the corresponding trace (bottom). The width of the gradient zone and distance between dashed lines = ~100 μm; scale bars = 100 μm.

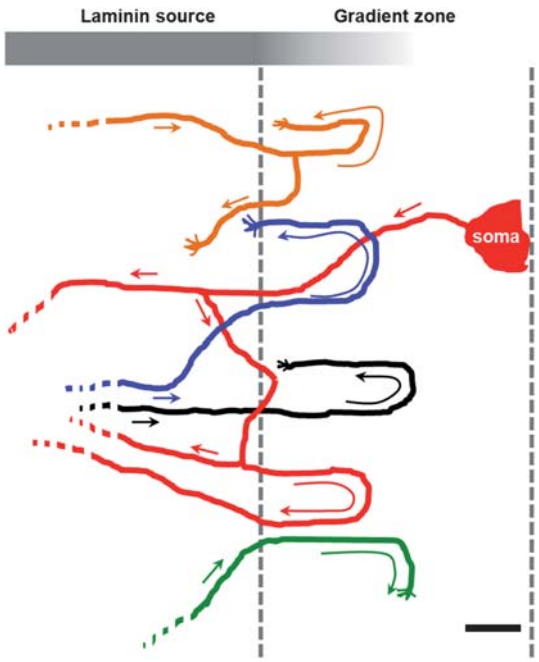

Fig. 4 Growing axons return to preferred laminin (LN) substrates. Traces of axons from hippocampal neurons cultured for 4 days on cover slips patterned and labeled with LN and FITC–PLL using a type B3 device (Fig. 2). Characteristic "U-turns" of axons are observed as the elongating axon discriminates lower LN concentrations and returns to the higher concentration of LN; relative substrate concentrations are shown above the neurite traces. Growth cones and arrows are added to signify the leading edge and the direction of migration and putative growth, respectively. The fragmented axonal portion represents the extensive axonal segment out of the field of view. The LN gradient zone is demarcated by the dashed lines, traces are from multiple samples and locations and are aligned to the gradient zone boundaries (dashed lines). Scale bar = 20 μm.

toward increasing laminin concentrations.[37] While linear gradients can influence which of the many neurites will become the axon, the authors also reported that linear gradients do not guide newly formed axons beyond the initial axon specification.[37] Since their analysis included only those neurons that were in the center of the linear gradient, the conclusions are limited to that sub-population.

By analyzing the neurons and neurites within the gradient zone, a broader perspective can be obtained. Halfter studied axons from retinal explants growing up and down merosin (a member of the LN protein family) gradients.[72] As a result, the axons generally grow straight, but at varying angles toward increased concentrations of merosin. The results are dependent upon the axon location with respect to the margins of the gradient zone. It was also shown that these sensory axons do not form U-turns in response to decreasing concentration gradients. Similar results were obtained from axons of chick sympathetic ganglia explants growing on LN gradients.[73] The relatively straight axon outgrowth observed in these studies is either an inherent property of the neurons,[74] a property of the substrate composition or a combined effect of these factors.

When taken together, our results demonstrate that axons from primary hippocampal neurons not only follow increasing LN concentrations, but that axons can meander toward or away from the increasing LN concentrations during elongation (Fig. 3d and e). Our data further show that axons survey their environment and respond to the instructive properties available in the local substratum, whereby small concentration changes in surface-bound gradients can orient elongating axons throughout development rather than only during axon specification. This latter finding is perhaps best supported by the observed "U-turns" produced by axons that sense decreasing LN concentrations and return to the preferred LN cue of the source channel (Fig. 4).

Our results also demonstrate the utility of the simplified approach adapted in this work to generate instructive surface gradients (Fig. 1 and 2). While microfluidics have been used extensively for generating fluid-phase chemical gradients, the work presented here produces surface-bound gradients without relying on complex surface chemistry to covalently tether activating protein substrates to the glass. Instead, the method patterns stable substrates through the initial flux-limited protein exposure to the glass surface. These gradients are stable in culture media for weeks and thus are suitable for more long-ranging studies of growth.

Combining diffusion field patterning with laminar flow for diffusion mixing

We employed diffusive mixing by combining diffusion and laminar flow to produce substrate-bound gradients. Fig. 5 demonstrates the patterned gradient profiles formed through the type-A1 compartmentalized microdevice (for dimensions, see Table 1). LN (central channel) and FITC–PLL (peripheral channels) were perfused through a 200 μm wide central channel by vacuum aspiration applied directly to the central channel outlet. As FITC–PLL passes through the interconnecting channels, laminar flow confines the FITC–PLL to the fluidic domain adjacent to the channel sidewalls and thus only allows gradient formation to be achieved through diffusive mixing (Fig. 5a–c).

To further refine the ability to pattern two-component gradients, a modified approach of diffusive mixing was employed within a 50 μm wide channel of device type-A3 (Table 1) to yield 30 μm wide counter-gradients (Fig. 5d and e). Here, one of the two peripheral channels was filled with TR–BSA while the remaining peripheral channel was filled with FITC–PLL. While the peripheral channels and interconnects were filled, the central channel remained dry due to high surface tension in the central channel at the end of the interconnects. To initiate diffusive mixing, PBS was then aspirated through the central channel to fill and perfuse the central channel. The dual opposing gradients observed here are the result of the combined effects of lateral diffusion and laminar flow of protein substrates into the target channel without the use of valves (Fig. 5d and e). Our present data demonstrate the ability to form diffusion-mediated, surface-bound gradients ranging from 50 μm wide (Fig. 5b, central interconnecting region) down to 25 μm wide (Fig. 5c, near the channel outlet). By applying this technique to smaller 50 μm wide channels, two counter gradients of substrates are formed on the glass surface; each chemical profile displays a ~30 μm wide overlapping gradient field of adsorbed proteins (Fig. 5d and e). As our data suggest, the passive pattern actuation strategy

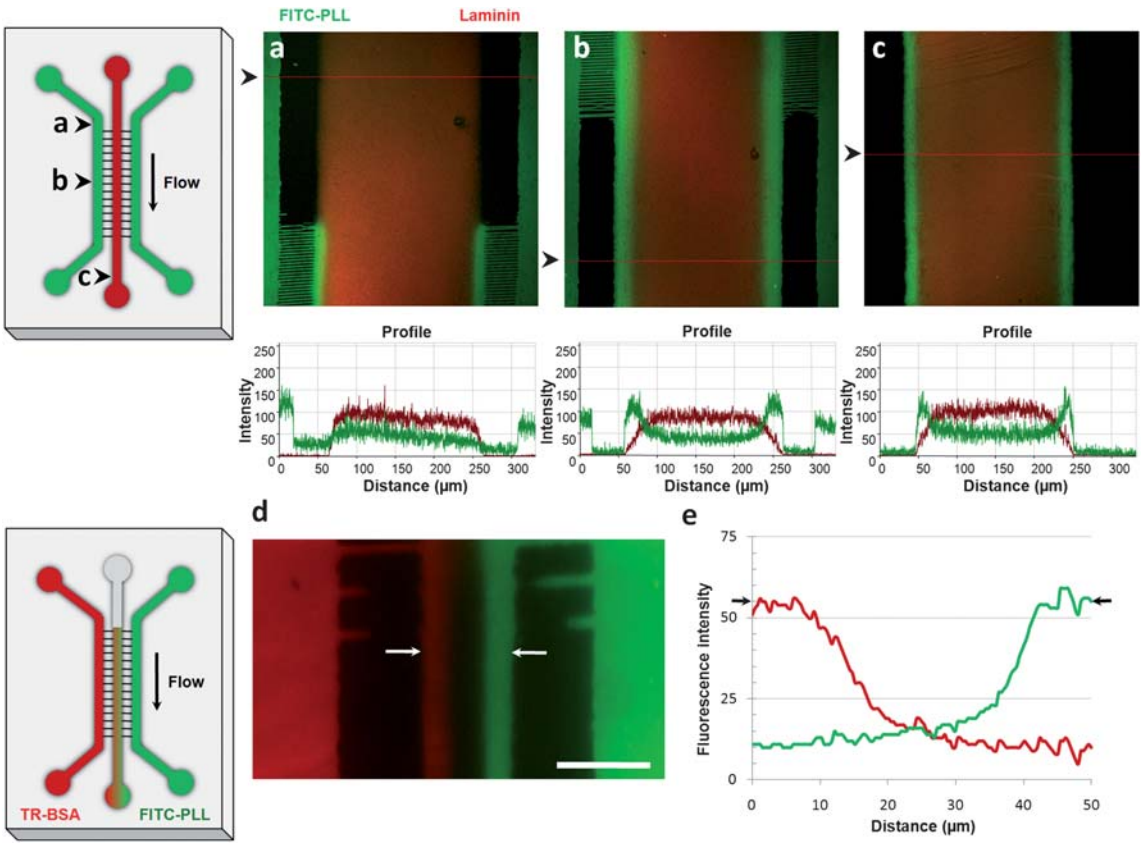

Fig. 5 Patterning planar gradients through combinations of laminar flow and diffusive mixing. (a–c) Schematic of microfluidic structure (device type A1) showing three points of analysis upstream, within and downstream of the micron-scale interconnecting channel region; substrates are: green = FITC–PLL, red = immunolabeled LN (Alexa 568 antibodies). (a) Center channel of a microfluidic device where two peripheral, parallel channels enable flow control into a center channel through micro-scale channel interconnects. This interconnected fluidic design permits the formation of chemically patterned gradient slopes (50 μm wide) adjacent to channel sidewalls. (b) Image and profile of fluorescently labeled substrates immediately downstream of interconnects; the FITC–PLL substrate is directed into the perpendicular interconnecting channels through diffusion, and then withdrawn *via* aspiration-mediated laminar flow. (c) Analysis of the gradient channel near the outlet by evaluating intensity of FITC–PLL fluorescence reveals a stable gradient profile (width and slope). (d) Patterning *via* diffusive mixing and laminar flow also was achieved in a 50 μm center channel (device type A3) to produce opposing gradients of TR–BSA and FITC–PLL; (d and e) arrows represent the point of fluorescence measurement shown in the profile.

supports a simple but broadly useful form of functional chemical patterning.

Gradients for refining neurite navigation

By extension, the exposure and rinsing steps of the patterning process described above can be rearranged into a two-part process using a microdevice with different channel dimensions (type B3, Table 1) to produce an instructive substrate gradient in a narrow central portion of the center target channel (Fig. 6). First, all channels were loaded with PBS, the peripheral channels were then exchanged for LN and FITC–PLL, followed by aspiration of the central channel and an extended period of LN and FITC–PLL exposure. In the final step, the fluid in the peripheral channels is changed back to PBS for an extended rinsing duration followed by microchannel removal for cell culture. As a result, a small gradient of LN and FITC–PLL is generated on the glass surface. This is sufficient to guide neurite navigation. Processes align along a higher concentration that confines neuronal processes and cell bodies to a ~15 μm wide region in the middle of the central channel (Fig. 6a and b). The polar histogram summarizes the directional navigation for all neuronal processes within 8 separate images, with each image containing 1–2 neuronal soma (Fig. S2†). Superimposed neuronal traces depict the degree of neuronal confinement to the gradient fields (Fig. 6b and c). Fig. 6d displays the mean value for all histographical 'wedges' within a 30° bin. Whereas the two bins for the longitudinal axes are statistically significant ($p \leq 0.0001$) from the remaining bins, the axial bins (*i.e.*, 90° and 120°) are not statistically different from each other, one-way analysis of variance (ANOVA), Bonferroni's multiple comparison *post hoc* test. Our results demonstrate the ability to utilize biochemical gradients to effectively confine the neuronal processes along a longitudinal region relative to the scale of the neuron.

While our diffusion-field substrate gradients prove compliant to the biological requirements of cultured neurons, fluid-phase flow-field gradients are dynamic and tunable,[18] each providing their respective benefits. Our past work has established the general competency of depletion field patterning,[56] as is adopted and modified in the present work, which actually embeds

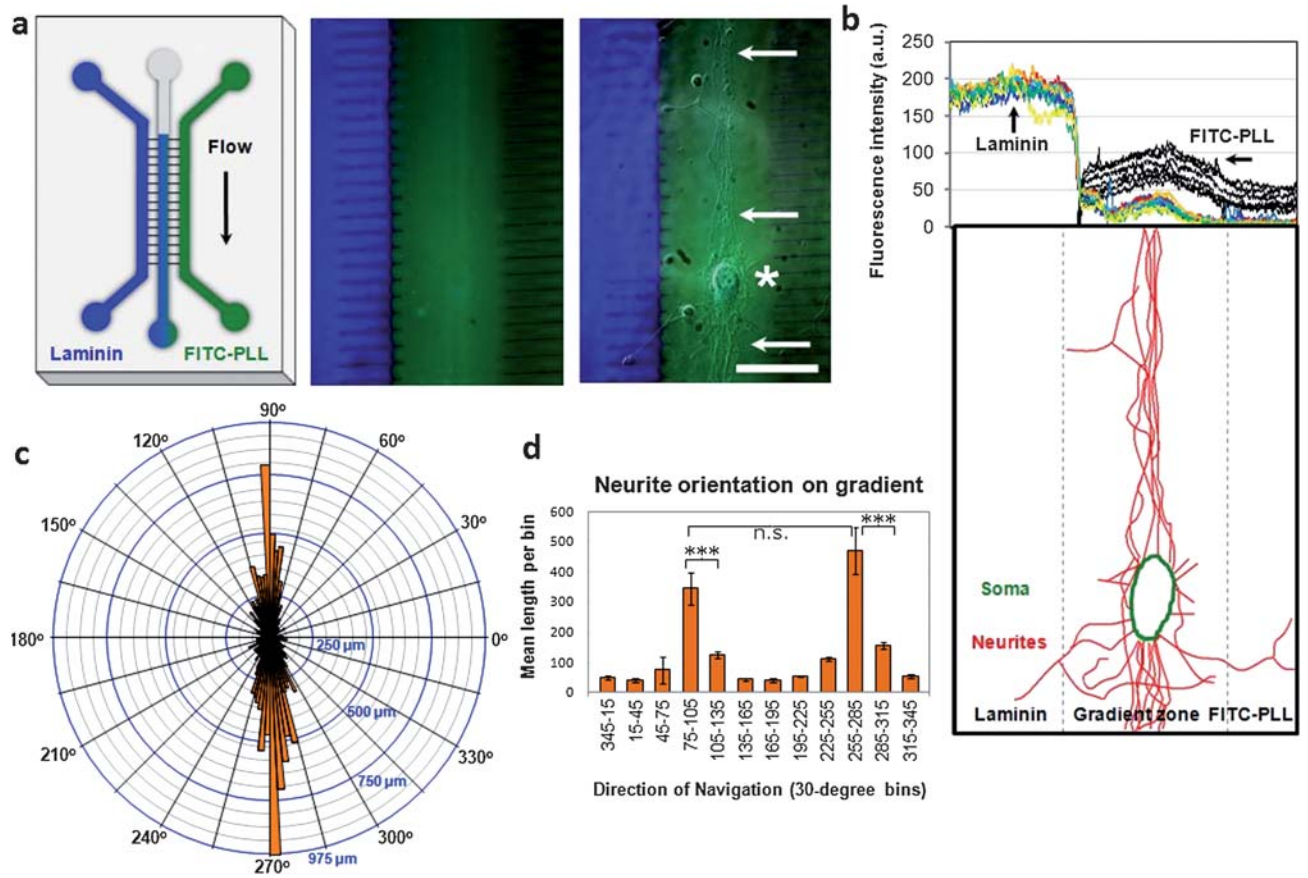

Fig. 6 Dual-layer substrate-gradients of LN and FITC–PLL guide neurite development. (a) Fluorescent image of a superimposed substrate gradient of LN and FITC–PLL formed through simultaneous flow of both substrates through the corresponding microdevice (type B3). Neurons were cultured on the combined gradient, live-cell and fluorescence imaging were performed to assess neurite navigation, scale bar is 50 µm. (a and b) Neuronal processes orient preferentially on the combined gradients of LN and FITC–PLL patterned in the central, 50 µm wide channel; neurites are constrained to a narrow region (~15 µm wide) of higher substrate concentrations, indicated by white arrows, asterisk (*) identifies soma. (b) Fluorescence profiles of the combined LN and FITC–PLL substrate gradients and the corresponding neurite traces of localized processes. (c) Polar histogram of all neurite traces from 8 separate images within the same sample. Each orange wedge represents the total length of all segments that extend in each angular direction; blue markers scale total length per wedge. (d) The means (±SEM) of all wedges for each 30° bin (*e.g.*, 345–15°) are displayed. The two bins for the longitudinal axis of the gradient (*i.e.*, 90° and 270°) are significantly different from all other bins, but are not statistically significant from each other, one-way ANOVA, $p \leq 0.0001$.

a significant advance in its capabilities. This model is one that we have theoretical guidance for and have replicated in a variety of contexts using different proteins and polycation adsorbates. Because each molecular compound has intrinsic properties of adhesion, each substrate compound of interest must be optimized, taking into consideration solution viscosity, molecular affinity to the binding surfaces, chemical substrate concentration, flow rate, time, temperature and the chemical properties of the physical surface to which the adsorbate is deposited.

Combined binary patterns and surface gradients for neuron development

To demonstrate the ability to form adlayers of differential substrate patterns that further guide neuron development, binary FITC–PLL lines were patterned on glass followed by an additional, perpendicular layer of TR–BSA and LN substrates (Fig. 7a and b). When neurons are seeded onto the FITC–PLL line where the LN and TR–BSA cues converge, axons are confined to the FITC–PLL line and are directed to extend in the direction of the LN substrate. Fig. 7 shows neurons on the three-component substrate formed through this sequential patterning process. Here, multi-layer lines and gradients in combination refine substrate-directed development through neurite confinement and guidance. While the combined lines and gradients presented here demonstrate a proof of principle for neurite confinement and developmental directionality, the channels and geometries used here are a low throughput approach. By applying these principles of substrate patterning to a larger microfluidic array—with channel sizes and architectures designed for large scale network formation—this approach could enable the ability to combine patterning techniques to provide a growth regimen for directing neuron polarity and connectivity. Work to this end will provide the precision required for defining neuronal polarity for studies ranging from subcellular substrate interactions to investigations of neural connectivity and repair.

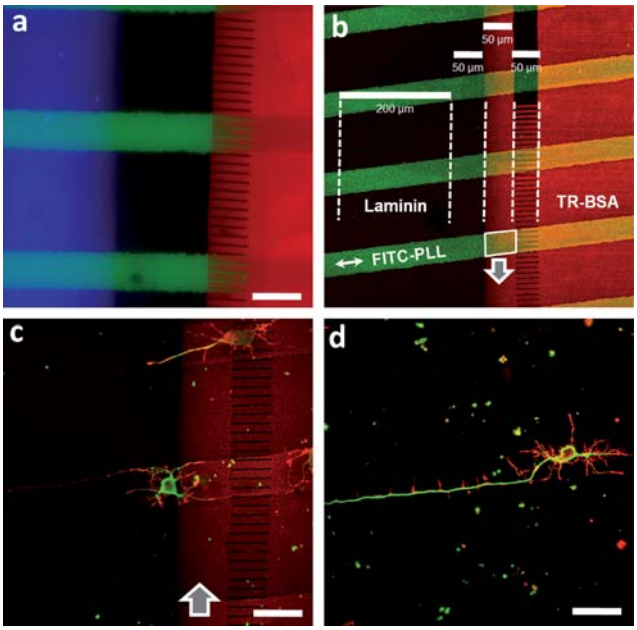

Fig. 7 The combination of binary lines and surface gradients increases substrate complexity. (a) A three-component pattern demonstrates the feasibility of sequential patterning processes and the biocompatibility of this more complex substrate. Two microfluidic devices with different channel architectures were used to pattern FITC–PLL (green) binary lines prior to patterning a second layer of parallel lines consisting of LN (blue) and TR–BSA (red) using device type B3. Immunochemistry was incorporated following the substrate patterning to provide the three-color label for fluorescence imaging. (b–d) In separate samples, binary lines and gradients were combined for neuron culture, labeled and imaged with confocal microscopy. (b) The LN source channel (labeled blue in (a)) is outlined with dashed lines and a 200 μm scale bar; the BSA patterns and interconnecting regions (red) also were determined in (a) and are outlined (dashed lines and 50 μm scale bars). The large arrow identifies the combined pattern of LN and TR–BSA, whereas the white box defines the region of a three component pattern (FITC–PLL, LN and TR–BSA). (c) Neurons cultured for 4 days were fixed and labeled with rhodamine-conjugated phalloidin for f-actin (red) and antibodies against α-tubulin (green). (d) A neuron on a binary FITC–PLL-patterned line outside gradient zone within the same culture shows the characteristic neuron morphology by developing a single, characteristically long process (axon) and several shorter branching processes (dendrites). (b and c) The large arrows mark the central channel gradient zone, a triple substrate-patterned area is formed in defined areas when the substrate gradient is patterned upon the binary patterns.

Conclusion

The cytoarchitecture of cultured neurons can be controlled by defining the surface chemistry of the substrate through microfluidic devices, a technology that enables the formation of biochemical surface gradients apart from, and in conjunction with, binary patterned cues. Because the PDMS channels can be discarded after surface gradient formation and prior to cell culture, the complexities surrounding experiments where rapid flow rates and shear stresses interfere with cell development can be avoided. When microfluidics are required, and flow regimens and shear stresses can be controlled within the desired cellular constraints, then the patterning approach presented here can complement and facilitate studies using patterned cultures within microfluidic channels.

The patterning approach presented here makes use of an interconnected channel design to achieve a broad range of substrate compositions that reveal cellular responses guiding the development of postnatal neurons. Our results show that diffusion-field gradients of LN can direct axon navigation beyond the initial axon specification. Specifically, when axons are exposed to both an adhesive cue (PLL) and an instructional cue (LN), then elongating neurites can sense changes in LN concentrations and turn to navigate toward the increasing LN concentration. Axons migrating down LN gradients are also observed forming "U-turns" and orient back toward higher laminin concentrations. In addition, growing neurites can be confined by narrow, superimposed gradients of LN and PLL for neuronal network engineering and studying the nervous system *in vitro*. This work further demonstrates the beneficial utilization of microfluidic devices for spatiotemporal delivery of instructive substrates for neurobiology, surface chemistry and bioengineering research.

Acknowledgements

This study was supported by the National Institute of Mental Health (R21 MH085220) (MUG) and NSF CHE0704153 (RGN). L. Millet was supported by the National Institute of Child Health and Human Development Developmental Psychobiology and Neurobiology Training Grant (HD007333). The content is solely the responsibility of the authors and does not necessarily represent the official views of the NIH or NSF.

References

1 A. M. Taylor, M. Blurton-Jones, S. W. Rhee, D. H. Cribbs, C. W. Cotman and N. L. Jeon, *Nat. Methods*, 2005, **2**, 599–605.
2 S. W. Rhee, A. M. Taylor, D. H. Cribbs, C. W. Cotman and N. L. Jeon, *Biomed. Microdevices*, 2007, **9**, 15–23.
3 F. Morin, N. Nishimura, L. Griscom, B. Lepioufle, H. Fujita, Y. Takamura and E. Tamiya, *Biosens. Bioelectron.*, 2006, **21**, 1093–1100.
4 A. M. Taylor, S. W. Rhee, C. H. Tu, D. H. Cribbs, C. W. Cotman and N. L. Jeon, *Langmuir*, 2003, **19**, 1551–1556.
5 G. N. Li, J. Liu and D. Hoffman-Kim, *Ann. Biomed. Eng.*, 2008, **36**, 889–904.
6 G. S. Withers, C. D. James, C. E. Kingman, H. G. Craighead and G. A. Banker, *J. Neurobiol.*, 2006, **66**, 1183–1194.
7 A. A. Oliva, Jr, C. D. James, C. E. Kingman, H. G. Craighead and G. A. Banker, *Neurochem. Res.*, 2003, **28**, 1639–1648.
8 T. Esch, V. Lemmon and G. Banker, *J. Neurosci.*, 1999, **19**, 6417–6426.
9 Y. Endo and J. S. Rubin, *Cancer Sci.*, 2007, **98**, 1311–1317.
10 G. Loers and M. Schachner, *J. Neurochem.*, 2007, **101**, 865–882.
11 D. W. Branch, J. M. Corey, J. A. Weyhenmeyer, G. J. Brewer and B. C. Wheeler, *Med. Biol. Eng. Comput.*, 1998, **36**, 135–141.
12 P. Shi, K. Shen and L. C. Kam, *Dev. Neurobiol.*, 2007, **67**, 1765–1776.
13 B. C. Wheeler, J. M. Corey, G. J. Brewer and D. W. Branch, *J. Biomech. Eng.*, 1999, **121**, 73–78.
14 J. M. Corey, B. C. Wheeler and G. J. Brewer, *J. Neurosci. Res.*, 1991, **30**, 300–307.
15 T. A. Kapur and M. S. Shoichet, *J. Biomater. Sci., Polym. Ed.*, 2003, **14**, 383–394.
16 T. A. Kapur and M. S. Shoichet, *J. Biomed. Mater. Res.*, 2004, **68a**, 235–243.
17 K. Moore, M. MacSween and M. Shoichet, *Tissue Eng.*, 2006, **12**, 267–278.
18 T. M. Keenan and A. Folch, *Lab Chip*, 2008, **8**, 34–57.
19 J. C. McDonald, D. C. Duffy, J. R. Anderson, D. T. Chiu, H. Wu, O. J. Schueller and G. M. Whitesides, *Electrophoresis*, 2000, **21**, 27–40.

20 J. M. Ng, I. Gitlin, A. D. Stroock and G. M. Whitesides, *Electrophoresis*, 2002, **23**, 3461–3473.
21 H. Shin, *Biomaterials*, 2007, **28**, 126–133.
22 J. Wang, L. Ren, L. Li, W. Liu, J. Zhou, W. Yu, D. Tong and S. Chen, *Lab Chip*, 2009, **9**, 644–652.
23 L. J. Millet, M. E. Stewart, J. V. Sweedler, R. G. Nuzzo and M. U. Gillette, *Lab Chip*, 2007, **7**, 987–994.
24 R. Morales, M. Riss, L. Wang, R. Gavin, J. A. Del Rio, R. Alcubilla and E. Claverol-Tinture, *Lab Chip*, 2008, **8**, 1896–1905.
25 D. R. Reyes, E. M. Perruccio, S. P. Becerra, L. E. Locascio and M. Gaitan, *Langmuir*, 2004, **20**, 8805–8811.
26 R. Gomez-Sjoberg, A. A. Leyrat, D. M. Pirone, C. S. Chen and S. R. Quake, *Anal. Chem.*, 2007, **79**, 8557–8563.
27 K. Jo, M. L. Heien, L. B. Thompson, M. Zhong, R. G. Nuzzo and J. V. Sweedler, *Lab Chip*, 2007, **7**, 1454–1460.
28 J. Liu, B. A. Williams, R. M. Gwirtz, B. J. Wold and S. Quake, *Angew. Chem., Int. Ed.*, 2006, **45**, 3618–3623.
29 J. S. Marcus, W. F. Anderson and S. R. Quake, *Anal. Chem.*, 2006, **78**, 3084–3089.
30 J. Melin and S. R. Quake, *Annu. Rev. Biophys. Biomol. Struct.*, 2007, **36**, 213–231.
31 E. A. Ottesen, J. W. Hong, S. R. Quake and J. R. Leadbetter, *Science*, 2006, **314**, 1464–1467.
32 M. Manthorpe, E. Engvall, E. Ruoslahti, F. M. Longo, G. E. Davis and S. Varon, *J. Cell Biol.*, 1983, **97**, 1882–1890.
33 T. S. Ford-Holevinski, J. M. Hopkins, J. P. McCoy and B. W. Agranoff, *Brain Res.*, 1986, **393**, 121–126.
34 J. M. Hopkins, T. S. Ford-Holevinski, J. P. McCoy and B. W. Agranoff, *J. Neurosci.*, 1985, **5**, 3030–3038.
35 A. D. Lander, D. K. Fujii and L. F. Reichardt, *J. Cell Biol.*, 1985, **101**, 898–913.
36 A. D. Lander, D. K. Fujii and L. F. Reichardt, *Proc. Natl. Acad. Sci. U. S. A.*, 1985, **82**, 2183–2187.
37 S. K. Dertinger, X. Jiang, Z. Li, V. N. Murthy and G. M. Whitesides, *Proc. Natl. Acad. Sci. U. S. A.*, 2002, **99**, 12542–12547.
38 S. L. Rogers, P. C. Letourneau, S. L. Palm, J. McCarthy and L. T. Furcht, *Dev. Biol.*, 1983, **98**, 212–220.
39 D. Edgar, R. Timpl and H. Thoenen, *EMBO J.*, 1984, **3**, 1463–1468.
40 B. G. Chung, L. A. Flanagan, S. W. Rhee, P. H. Schwartz, A. P. Lee, E. S. Monuki and N. L. Jeon, *Lab Chip*, 2005, **5**, 401–406.
41 G. A. Cooksey, C. G. Sip and A. Folch, *Lab Chip*, 2009, **9**, 417–426.
42 J. Diao, L. Young, S. Kim, E. A. Fogarty, S. M. Heilman, P. Zhou, M. L. Shuler, M. Wu and M. P. DeLisa, *Lab Chip*, 2006, **6**, 381–388.
43 R. C. Gunawan, J. Silvestre, H. R. Gaskins, P. J. Kenis and D. E. Leckband, *Langmuir*, 2006, **22**, 4250–4258.
44 R. F. Ismagilov, T. D. Rosmarin, J. A. Kenis, D. T. Chiu, W. Zhang, H. A. Stone and G. M. Whitesides, *Anal. Chem.*, 2001, **73**, 4682–4687.
45 N. L. Jeon, S. K. W. Dertinger, D. T. Chiu, I. S. Choi, A. D. Stroock and G. M. Whitesides, *Langmuir*, 2000, **16**, 8311–8316.
46 C. Couzon, A. Duperray and C. Verdier, *Eur. Biophys. J.*, 2009, **38**, 1035–1047.
47 L. Kim, Y. C. Toh, J. Voldman and H. Yu, *Lab Chip*, 2007, **7**, 681–694.
48 H. S. Shin, H. J. Kim, S. J. Sim and N. L. Jeon, *J. Nanosci. Nanotechnol.*, 2009, **9**, 7330–7335.
49 G. M. Walker, H. C. Zeringue and D. J. Beebe, *Lab Chip*, 2004, **4**, 91–97.
50 C. J. Wang, X. Li, B. Lin, S. Shim, G. L. Ming and A. Levchenko, *Lab Chip*, 2008, **8**, 227–237.
51 O. Thoumine, R. M. Nerem and P. R. Girard, *Lab. Invest.*, 1995, **73**, 565–576.
52 O. Thoumine, R. M. Nerem and P. R. Girard, *In Vitro Cell. Dev. Biol.: Anim.*, 1995, **31**, 45–54.
53 O. Thoumine, T. Ziegler, P. R. Girard and R. M. Nerem, *Exp. Cell Res.*, 1995, **219**, 427–441.
54 J. Wang, J. Heo and S. Z. Hua, *Lab Chip*, 2010, **10**, 235–239.
55 I. Caelen, A. Bernard, D. Juncker, B. Michel, H. Heinzelmann and E. Delamarche, *Langmuir*, 2000, **16**, 9125–9130.
56 K. A. Fosser and R. G. Nuzzo, *Anal. Chem.*, 2003, **75**, 5775–5782.
57 W. Saadi, S. W. Rhee, F. Lin, B. Vahidi, B. G. Chung and N. L. Jeon, *Biomed. Microdevices*, 2007, **9**, 627–635.
58 S. Paliwal, P. A. Iglesias, K. Campbell, Z. Hilioti, A. Groisman and A. Levchenko, *Nature*, 2007, **446**, 46–51.
59 T. M. Keenan, C. H. Hsu and A. Folch, *Appl. Phys. Lett.*, 2006, **89**, 114103(1-3).
60 A. L. Briseno, M. Roberts, M. M. Ling, H. Moon, E. J. Nemanick and Z. Bao, *J. Am. Chem. Soc.*, 2006, **128**, 3880–3881.
61 G. Y. Choi, S. Kim and A. Ulman, *Langmuir*, 1997, **13**, 6333–6338.
62 K. Glasmästar, J. Gold, A. S. Andersson, D. S. Sutherland and B. Kasemo, *Langmuir*, 2003, **19**, 5475–5483.
63 D. J. Graham, D. D. Price and B. D. Ratner, *Langmuir*, 2002, **18**, 1518–1527.
64 X. M. Li, M. Péter, J. Huskens and D. N. Reinhoudt, *Nano Lett.*, 2003, **3**, 1449–1453.
65 T. P. Sullivan, M. L. van Poll, P. Y. Dankers and W. T. Huck, *Angew. Chem., Int. Ed.*, 2004, **43**, 4190–4193.
66 X. Wang, M. Östblom, T. Johansson and O. Inganäs, *Thin Solid Films*, 2004, **449**, 125–132.
67 K. Felmet, Y. L. Loo and Y. Sun, *Appl. Phys. Lett.*, 2004, **85**, 3316–3318.
68 P. S. Hale, P. Kappen, W. Prissanaroon, N. Brack, P. J. Pigram and J. Liesegang, *Appl. Surf. Sci.*, 2007, **253**, 3746–3750.
69 R. B. A. Sharpe, D. Burdinski, C. van der Marel, J. A. J. Jansen, J. Huskens, H. J. W. Zandvliet, D. N. Reinhoudt and B. Poelsema, *Langmuir*, 2006, **22**, 5945–5951.
70 C. Thibault, C. Severac, A. F. Mingotaud, C. Vieu and M. Mauzac, *Langmuir*, 2007, **23**, 10706–10714.
71 T. B. Kuhn, C. V. Williams, P. Dou and S. B. Kater, *J. Neurosci.*, 1998, **18**, 184–194.
72 W. Halfter, *J. Neurosci.*, 1996, **16**, 4389–4401.
73 M. P. McKenna and J. A. Raper, *Dev. Biol.*, 1988, **130**, 232–236.
74 W. Halfter, D. F. Newgreen, J. Sauter and U. Schwarz, *Dev. Biol.*, 1983, **95**, 56–64.